

Extended staggered-flux phases in two-dimensional lattices

Yi-Fei Wang¹ Chang-De Gong^{2,3,4} and Shi-Yao Zhu³

¹National Laboratory of Solid State Microstructures and Department of Physics, Nanjing University, Nanjing 210093, China

²Chinese Center of Advanced Science and Technology (World Laboratory), P.O. Box 8730, Beijing 100080, China

³Department of Physics, Hong Kong Baptist University, Kowloon Tong, Hong Kong, China

⁴Department of Physics, The Chinese University of Hong Kong, Hong Kong, China

(Dated: August 24, 2018)

Based on the so called t - ϕ model in two-dimensional (2D) lattices, we investigate the stabilities of a class of extended staggered-flux (SF) phases (which are the extensions of the $\sqrt{2} \times \sqrt{2}$ SF phase to generalized spatial periods) against the Fermi-liquid phase. Surprisingly, when away from the nesting electron filling, some extended-SF phases take over the dominant SF phase (the $\sqrt{2} \times \sqrt{2}$ SF phase for the square lattice, a $1 \times \sqrt{3}$ SF phase for the triangular one), compete with the Fermi-liquid phase in nontrivial patterns, and still occupy significant space in the phase diagram through the advantage in the total electronic kinetic energies. The results can be termed as the generalized Perierls orbital-antiferromagnetic instabilities of the Fermi-liquid phase in 2D lattice-electron models.

PACS numbers: 71.70.-d, 75.10.-b, 75.10.Lp, 71.10.Hf

I. INTRODUCTION

An intriguing orbital-current-carrying state in the square lattice, the staggered-flux (SF) phase¹ (also known as orbital antiferromagnet², d -density wave³ state, or charge flux phase) which has the spatial period $\sqrt{2} \times \sqrt{2}$, has been the focus of consideration for a long time. This $\sqrt{2} \times \sqrt{2}$ SF phase was first considered in excitonic insulators², then in high- T_c superconductors¹. The absence of experimental vindications made it discarded in favor of other conventional orders. Recently, it regains new attentions since unusual experimental findings in two systems: a hidden order in the heavy-fermion compound URu₂Si₂⁴; a pseudogap phenomena (See the review by Timusk *et al.*⁵) in the underdoped region of high- T_c cuprates³.

In parallel with the experimental contexts, numerical signatures in the t - J model^{6,7} and evidences in two-leg ladder models (half-filled t - U - V - J ⁸, doped t - J - V - V' and t - J_{\perp} - U - V_{\perp} ⁹) of its existence have been found. It is also being discussed now in many new theoretical contexts: the double-exchange model¹⁰ of colossal-magnetoresistance manganites; the repulsive SU(N) Hubbard Model¹¹ of ultracold fermionic atoms in optical lattices; models with ring-exchange interactions¹².

For the triangular lattice case, a $1 \times \sqrt{3}$ SF phase with $\pi/2$ -flux per plaquette has been considered as the mean-field ansatz¹³ for the Heisenberg model. Recently found layered sodium cobalt oxide system Na _{x} CoO₂yH₂O¹⁴ makes it a reasonable reference state for a range of electron filling¹⁵.

To the best of our knowledge, the formal exploration of other possible staggered-flux phases has never been made in previous studies (except a suggestion in studying the double-exchange model¹⁰). We would address the following problems: can a class of extended-SF phases with generalized spatial periods, which are still macroscopically space-inversion and time-reversal invariant, be

stabilized in a 2D lattice-electron model? if so, how do these extended-SF phases compete with each other and with the Fermi-liquid phase? is this kind of stabilization a generic feature of 2D lattice-electron models?

In this report, we try to answer the above questions through numerical studies of a class of extended-SF phases in the so-called t - ϕ model¹⁶ which is the simplest one being able to generate the $\sqrt{2} \times \sqrt{2}$ SF phase spontaneously. This model has also been shown¹⁷ to be closely related to the large- N SU(N) t - J model (where the $\sqrt{2} \times \sqrt{2}$ SF phase is first realized as a ground state¹) and the weak-coupling Hubbard model. If the idea about extended-SF phases can be realized in this simple model, then it should be further taken into account and be tested in the future studies of other more realistic models.

For each extended-SF phase, we first investigate the variation of the total kinetic energy (TKE) of tight-binding electrons (electron-hopping part of the t - ϕ model) versus the flux parameter ϕ . Further, including the “magnetic” energy of the flux itself, quantum phase transitions among these extended-SF phases and the Fermi-liquid phase are discussed in details through quantum phase diagrams.

II. NOTATION AND FORMULATION

The notation for an extended-SF phase is generally written as SF _{$r \times s$} ^L, where L=S,T represent the square lattice and the triangular one, respectively, and $r \times s$ represents the spatial period (*i.e.*, the size of a selected unit cell). Sometimes a Greek letter is added in the notation to distinguish among the extended-SF phases which have the same spatial period (*e.g.* SF _{$1 \times \sqrt{3}, \alpha$} ^T and SF _{$1 \times \sqrt{3}, \beta$} ^T). We will consider 8 kinds of extended-SF phases in each lattice. The flux configurations of various extended-SF phases are illustrated in Fig. 1. These extended-SF phases are chosen by examining their symmetries and

simplicities. More complicated extended-SF phases can also be obtained by the generalized routines, however, they have less importance both theoretically and experimentally.

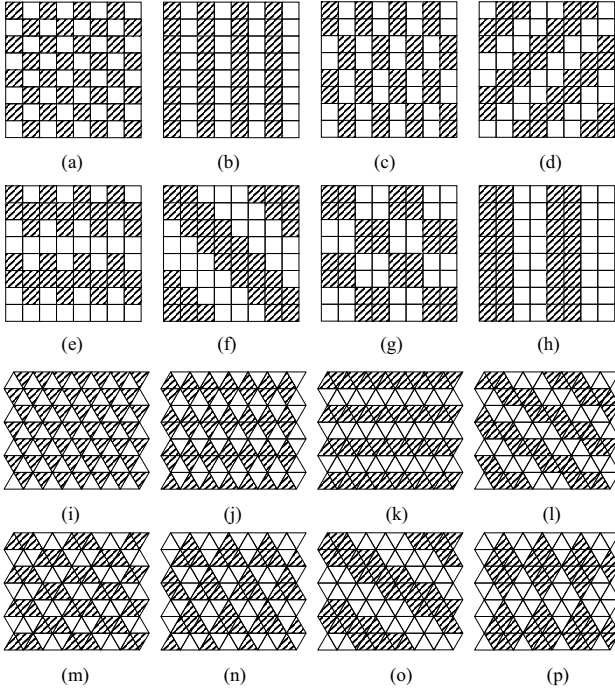


FIG. 1: Illustration of extended-SF phases in 2D lattices. Shaded plaquette has a flux $-\phi$, and the blank one has a flux ϕ . (a) $\text{SF}_{\sqrt{2} \times \sqrt{2}}^S$; (b) $\text{SF}_{1 \times 2}^S$; (c) $\text{SF}_{2 \times \sqrt{5}}^S$; (d) $\text{SF}_{\sqrt{2} \times 2\sqrt{2}}^S$; (e) $\text{SF}_{2 \times 4}^S$; (f) $\text{SF}_{\sqrt{2} \times 3\sqrt{2}}^S$; (g) $\text{SF}_{2\sqrt{2} \times 2\sqrt{2}}^S$; (h) $\text{SF}_{1 \times 4}^S$; (i) $\text{SF}_{1 \times 1}^T$; (j) $\text{SF}_{1 \times \sqrt{3}, \alpha}^T$; (k) $\text{SF}_{1 \times \sqrt{3}, \beta}^T$; (l) $\text{SF}_{\sqrt{3} \times 2}^T$; (m) $\text{SF}_{\sqrt{3} \times \sqrt{3}}^T$; (n) $\text{SF}_{2 \times 2}^T$; (o) $\text{SF}_{\sqrt{3} \times 3}^T$; (p) $\text{SF}_{2 \times 2\sqrt{3}}^T$.

The following U(1) gauge-invariant tight-binding Hamiltonian describes the t - ϕ model¹⁶:

$$H = -t \sum_{\langle ij \rangle \sigma} \left(e^{i\phi_{ij}} c_{j\sigma}^\dagger c_{i\sigma} + \text{H.c.} \right) + \frac{1}{2} K \sum_p \phi_p^2. \quad (1)$$

Here ϕ_{ij} is in units of $\phi_0/2\pi$ ($\phi_0 = hc/e$ is the flux quantum). The nearest-neighbor hopping integral of electrons t is modified as $t_{ij} = t \exp(i\phi_{ij})$ due to the Aharonov-Bohm effect. The second term of Eq. (1) gives the “magnetic” energy. ϕ_p is the sum of ϕ_{ij} (clockwisely) along a plaquette p . To capture the major physics, the spatial fluctuation of $|\phi_p|$ is neglected.

For each extended-SF phase, after taking a specific gauge (physical quantities are gauge-invariant as demonstrated before¹⁸), the first part of Eq. (1) can be converted to k -space and then be directly diagonalized, leads to several subbands of the energy spectrum. The symmetries of the extended-SF phases in Fig. 1 ensure that the number of subbands are not too large. Among these extended-SF phases, the energy spectra of three simpler ones, $\text{SF}_{\sqrt{2} \times \sqrt{2}}^S$ ^{16,18}, $\text{SF}_{1 \times 1}^T$ and $\text{SF}_{1 \times \sqrt{3}, \alpha}^T$ ¹⁹, have been clarified in details before.

After getting the energy spectrum (numerically for large Hamiltonian matrices), the total density of states (DOS) $D(\omega)$ can be obtained by summing up the contributions from all subbands. Thus the TKE per site for electron-filling factor ν at zero temperature is given by

$$E_{kin}(\phi, \nu) = \int_{\omega_{min}}^{\mu} d\omega D(\omega) \omega. \quad (2)$$

And the chemical potential μ is determined through

$$\nu = \int_{\omega_{min}}^{\mu} d\omega D(\omega). \quad (3)$$

Where ω_{min} is the lower limit of the energy spectrum. Both the DOS and TKE are invariant under the transformations $\phi \rightarrow -\phi$ and $\phi \rightarrow 2\pi - \phi$. Therefore, it is enough to consider E_{kin} for $0 \leq \phi \leq \pi$. For $\phi = 0$ (the Fermi-liquid phase) or π (also called the π -flux phase¹ in the square lattice), all extended-SF phases in a 2D lattice are equivalent and hence have the same E_{kin} .

Then through the self-consistent determination of the flux parameter ϕ by minimizing the total energy per site determined by the t - ϕ model (TKE plus the “magnetic” energy), we can plot the phase diagram in the ν - K parameter space by labelling the lowest-energy phase (an extended-SF phase or the Fermi-liquid phase) in the ν - K parameter space. Therefore for a given electron-filling factor ν , quantum phase transitions may occur when K changes, and vice versa.

III. SQUARE LATTICE

In Fig. 2 we plot the TKE per site versus the flux parameter ϕ for several values of electron filling ν 's. Due to the particle-hole symmetry in the square lattice, the DOS always has the property $D(\omega) = D(-\omega)$, and we have $E_{kin}(\phi, \nu) = E_{kin}(\phi, 1 - \nu)$. Hence E_{kin} - ϕ curves are plotted only for $\nu \leq 1/2$.

At $\nu = 1/2$ (Fig. 2(a)), $\text{SF}_{\sqrt{2} \times \sqrt{2}}^S$ has lower TKE than the Fermi-liquid phase ($\phi = 0$) and all other extended-SF phases for a given ϕ . That is why $\text{SF}_{\sqrt{2} \times \sqrt{2}}^S$ can be stabilized before^{1,16} near half filling. While at $\nu = 3/8$ (Fig. 2(b)) and even smaller filling factors, $\text{SF}_{\sqrt{2} \times \sqrt{2}}^S$ has higher TKE than all other extended-SF phases for a given ϕ . At $\nu = 3/8$, for $0 < \phi < 0.83$, $0.83 < \phi < 1.51$, and $1.51 < \phi < 3.14$, $\text{SF}_{2 \times \sqrt{5}}^S$, $\text{SF}_{2\sqrt{2} \times 2\sqrt{2}}^S$ and $\text{SF}_{1 \times 4}^S$ have the lowest TKE, respectively.

The nesting property of the Fermi surface in the Fermi-liquid phase at $\nu = 1/2$ makes the system resemble a one-dimensional Perierls system in which a lattice distortion lowers the TKE of electrons by opening a gap near the Fermi energy. Therefore the advantage of extended-SF phases versus the Fermi-liquid phase in TKE can be considered as the generalized Perierls orbital-antiferromagnetic instabilities¹⁶ of the Fermi-liquid phase near the nesting filling, similar to

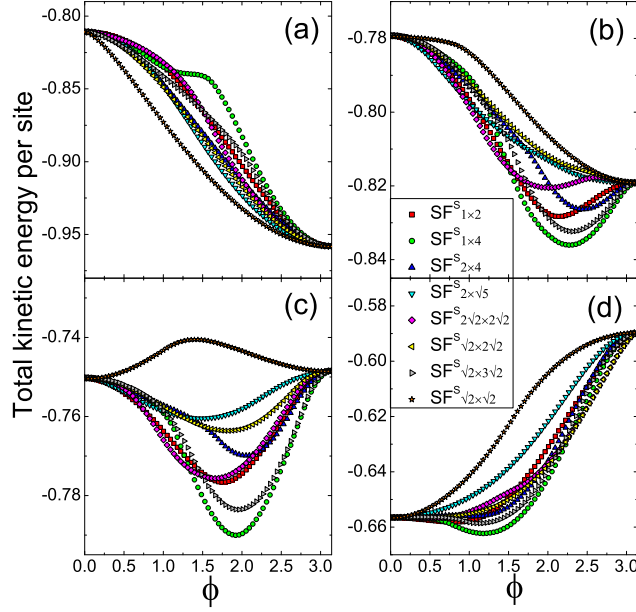


FIG. 2: (color online). Square lattice: total kinetic energy per site (in units of t) of extended-SF phases versus the flux parameter ϕ (in units of $\phi_0/2\pi$) for several values of electron filling ν 's. (a) $\nu = 1/2$; (b) $\nu = 3/8$; (c) $\nu = 1/3$; (d) $\nu = 1/4$.

the instability of lattice electrons in a uniform magnetic field²⁰. While away from the nesting filling, the advantage of extended-SF phases in TKE is weakened gradually. As for $\nu < 1/4$, nearly all extended-SF phases have higher TKE than the Fermi-liquid phase.

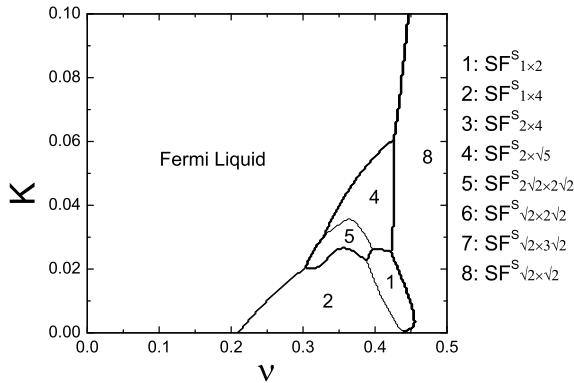


FIG. 3: Square lattice: phase diagram in the ν - K parameter space (K is in units of t).

The phase diagram in the ν - K parameter space is shown in Fig. 3. We notice that $\text{SF}_{2\times 4}^S$, $\text{SF}_{\sqrt{2}\times 2\sqrt{2}}^S$ and $\text{SF}_{\sqrt{2}\times 3\sqrt{2}}^S$ occupy no space in the phase diagram. At $\nu < 0.21$, the Fermi-liquid phase is robust against all extended-SF phases considered. When ν increases, $\text{SF}_{1\times 4}^S$ appears in the $K < 0.03t$ region. For $0.3 < \nu < 0.425$ and $K < 0.06t$, $\text{SF}_{1\times 2}^S$, $\text{SF}_{1\times 4}^S$, $\text{SF}_{2\times \sqrt{5}}^S$

and $\text{SF}_{2\sqrt{2}\times 2\sqrt{2}}^S$ compete and show several tricritical points. At $K > 0.06t$, only $\text{SF}_{\sqrt{2}\times \sqrt{2}}^S$ competes with the Fermi-liquid phase near half filling. If more complicated extended-SF phases are taken into account, the phase space will be divided into smaller portions, however, the general features should not be altered fundamentally.

The previous numerical studies^{6,7,8,9} suggest that the $\text{SF}_{\sqrt{2}\times \sqrt{2}}^S$ phase is a key ingredient of the ground state in the models of strongly correlated electrons, at least in the low doping regime (doping $x < 10\%$, *i.e.*, $0.45 < \nu < 0.5$), is in agreement with our results. And our results also suggest that when $\nu \leq 0.425$ (doping $x \geq 15\%$), the $\text{SF}_{\sqrt{2}\times \sqrt{2}}^S$ phase does not predominate; when $0.425 < \nu < 0.45$ (doping $10\% < x < 15\%$), stripe-like extended-SF phases, $\text{SF}_{1\times 2}^S$ and $\text{SF}_{1\times 4}^S$ should be taken as additional competitive ingredients of the ground state. Of course, in order to give quantitative evaluation of the TKE or the total free energy of interacting electrons, the hopping integral t should be renormalized by many-body effects.

It has been shown before that the instabilities of the Fermi-liquid phase in the t - ϕ model at nonzero K/t can be related to those in the large- N $\text{SU}(N)$ t - J model at nonzero t/J ¹⁷. Therefore the phase diagram in Fig. 3 which shows different Perierls orbital-antiferromagnetic instabilities at different electron fillings can be used to predict the existence of similar instabilities in the latter model.

IV. TRIANGULAR LATTICE

For the triangular lattice, the DOS has the symmetry $D(\omega, \pi - \phi) = D(-\omega, \phi)$ ¹⁹, consequently, $E_{kin}(\phi, \nu) = E_{kin}(\pi - \phi, 1 - \nu)$. Around the nesting filling $\nu = 3/4$, the extended-SF phases also exhibit the generic advantage in TKE versus the Fermi-liquid phase in broad ν - ϕ parameter space (see Fig. 4).

To obtain the phase diagram as shown in Fig. 5, one should notice that the “magnetic” energy per site is $K\phi^2$ in the triangular lattice (in which the number of plaquettes doubles the number of sites). $\text{SF}_{\sqrt{3}\times \sqrt{3}}^T$ does not appear in the phase diagram. For $\nu > 0.82$ and $K < 0.26t$, $\text{SF}_{1\times 1}^T$ dominates the phase space. For $K < 0.08t$ and ν close to the nesting filling $\nu = 3/4$, $\text{SF}_{2\times 2}^T$, $\text{SF}_{2\times 2\sqrt{3}}^T$ and $\text{SF}_{\sqrt{3}\times 3}^T$ compete. When ν is far away from the nesting filling ($\nu < 0.27$), the Fermi-liquid phase is robust against all extended-SF phases considered. For larger K ($K > 0.26t$), only $\text{SF}_{1\times \sqrt{3}, \alpha}^T$ is still robust against Fermi-liquid around $\nu = 3/4$. It suggests that in parallel with the importance of $\text{SF}_{\sqrt{2}\times \sqrt{2}}^S$ near half-filling in the square lattice, $\text{SF}_{1\times \sqrt{3}, \alpha}^T$ should be a key ingredient of the ground state in some lattice-electron models¹⁵ in the triangular lattice near $\nu = 3/4$.

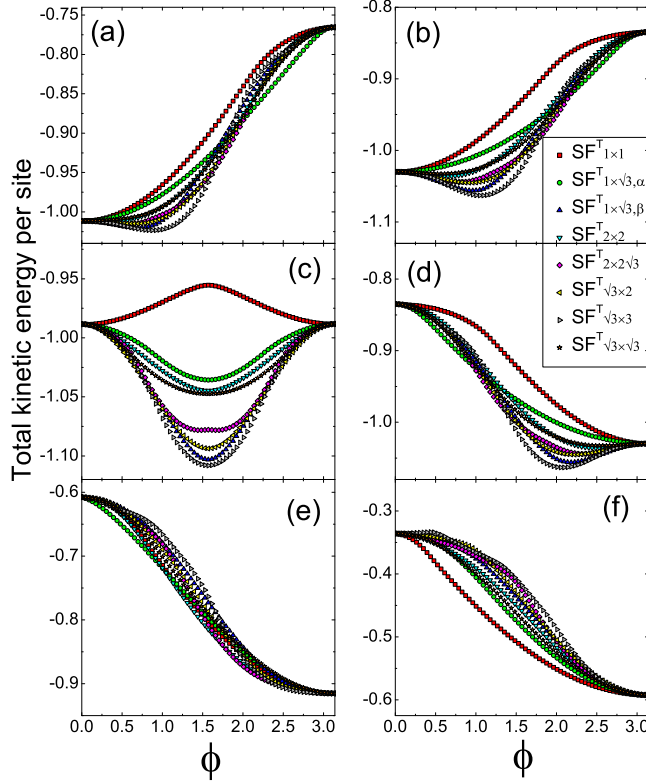


FIG. 4: (color online). Triangular lattice: total kinetic energy per site (in units of t) of extended-SF phases versus the flux parameter ϕ (in units of $\phi_0/2\pi$) for various values of electron filling ν 's. (a) $\nu = 1/3$; (b) $\nu = 3/8$; (c) $\nu = 1/2$; (d) $\nu = 5/8$; (e) $\nu = 3/4$; (f) $\nu = 7/8$.

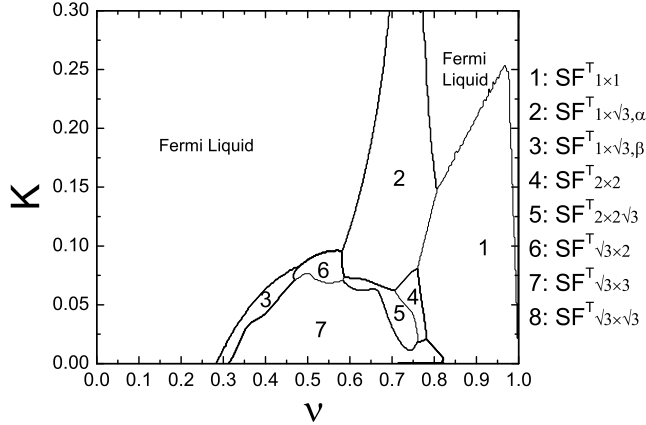


FIG. 5: Triangular lattice: phase diagram in the ν - K parameter space (K is in units of t).

V. SUMMARY AND CONCLUSIONS

In numerous works, the $\text{SF}^{\text{S}}_{\sqrt{2} \times \sqrt{2}}$ phase competes with other better-known phases, such as the phases of charge-density waves, spin-density waves, superconductivity, stripes and Fermi liquid in the square lattice. The possibilities of other extended-SF phases in both the square lattice and the triangular one, and the competition among these extended-SF phases and the Fermi-liquid phase, which have never been considered before, are the main contributions of this report.

In conclusion, there are several points to be addressed: (a) the generic and strong electron-filling-dependent stabilization of extended-SF phases in some parameter space of the simple t - ϕ model is an illustration of generalized Perierls orbital-antiferromagnetic instabilities of the Fermi-liquid phase in 2D lattices; (b) in the square lattice, the $\text{SF}^{\text{S}}_{\sqrt{2} \times \sqrt{2}}$ phase is dominantly robust close to half filling, which agrees with previous studies; (c) away from half filling, other extended-SF phases are possible as a result of advantage in TKE against the Fermi-liquid phase; (d) in the triangular lattice, we find the $\text{SF}^{\text{T}}_{1 \times \sqrt{3}, \alpha}$ phase is robust around the nesting filling $\nu = 3/4$ (in a manner similar to the $\text{SF}^{\text{S}}_{\sqrt{2} \times \sqrt{2}}$ phase in the square lattice), and other extended-SF phases are also possible when ν is away from $3/4$; (e) since lowering TKE of electrons plays an decisive role in minimizing the total mean-field free energy in many cases, we keep cautious but optimistic hopes about applying our nontrivial new results based on a simple model to other more realistic systems such as the t - J model and its large- N limit, the Hubbard or extended Hubbard model and their weak-coupling limits or large- N limits, the double-exchange model and models with ring-exchange interactions.

This work is supported by the Chinese National Natural Science Foundation and RGC of HK Government, and FRG of HKBU.

¹ I. Affleck and J. B. Marston, Phys. Rev. B **37**, R3774 (1988); J. B. Marston and I. Affleck, *ibid.*, **39**, 11538 (1989).
² B. I. Halperin and T. M. Rice, Solid State Phys. **21**, 115 (1968).
³ S. Chakravarty, R. B. Laughlin, D. K. Morr, and C. Nayak, Phys. Rev. B **63**, 094503 (2001).

⁴ P. Chandra, P. Coleman, J. A. Mydosh, and V. Tripathi, Nature (London) **417**, 831 (2002).
⁵ T. Timusk and B. Statt, Rep. Prog. Phys. **62**, 61 (1999).
⁶ D. A. Ivanov, P. A. Lee, and X.-G. Wen, Phys. Rev. Lett. **84**, 3958 (2000).
⁷ P. W. Leung, Phys. Rev. B **62**, R6112 (2000).

- ⁸ J. B. Marston and J. O. Fjærestad and A. Sudbø, Phys. Rev. Lett. **89**, 056404 (2002).
- ⁹ U. Schollwöck, S. Chakravarty, J. O. Fjærestad, J. B. Marston, and M. Troyer, Phys. Rev. Lett. **90**, 186401 (2003)
- ¹⁰ M. Yamanaka, W. Koshibae, and S. Maekawa, Phys. Rev. Lett. **81**, 5604 (1998).
- ¹¹ C. Honerkamp and W. Hofstetter Phys. Rev. Lett. **92**, 170403 (2004).
- ¹² C. H. Chung, H. Y. Kee and Y. B. Kim, Phys. Rev. B **67**, 224405 (2003); B. Normand and A. M. Oleś *ibid*, **70**, 134407 (2004).
- ¹³ T. K. Lee and Shiping Feng, Phys. Rev. B **41**, 11110 (1990).
- ¹⁴ K. Takada *et al.*, Nature (London) **422**, 53 (2003)
- ¹⁵ G. Baskaran, Phys. Rev. Lett. **91**, 097003 (2003).
- ¹⁶ A. B. Harris, T. C. Lubensky and E. J. Mele, Phys. Rev. B **40**, R2631 (1989).
- ¹⁷ D. C. Morse and T. C. Lubensky, Phys. Rev. B, **42**, 7994 (1990).
- ¹⁸ J. An, C. D. Gong, and H. Q. Lin, Phys. Rev. B **63**, 174434 (2001).
- ¹⁹ Y. F. Wang, C. D. Gong and S. Y. Zhu, Europhys. Lett. **69**, 404 (2005).
- ²⁰ Y. Hasegawa, P. Lederer, T. M. Rice and P. B. Wiegmann Phys. Rev. Lett. **63**, 907 (1989).